Journal of Applied Polymer Science

Organic Solvent Nanofiltration with a Poly(dimethylsiloxane) Membrane: Parameters Affecting its Sieving Properties

Loïc Leitner, Christelle Harscoat-Schiavo, Romain Kapel, Cécile Vallieres
LRGP (CNRS UMR7274) Université de Lorraine, Nancy 54001, France
Correspondence to: C. Vallieres (E-mail: cecile.vallieres@univ-lorraine.fr)

ABSTRACT: In this study, retention experiments were performed to characterize the variable sieving properties of a poly(dimethylsiloxane) (PDMS) membrane in relation with operating parameters. The swelling, transmembrane pressure, and temperature are all known to impact the physicochemical properties and morphology of PDMS polymer and were therefore varied for the purposes of our retention experiments which assessed them with the homologous series of polyethylene glycols (PEGs; 200–1500 g mol^{-1}). The objectives were twofold—first, to evaluate the capacity to induce a targeted molecular weight cutoff (MWCO) by selecting appropriate filtration conditions and second to better understand the mechanisms involved during solvent-resistant nanofiltration with PDMS. The selected solvents or solvent/solvent mixtures used throughout this study were found to induce swelling ratios of 1.16 (ethanol/ethyl acetate: 25/75), 1.26 (ethyl acetate), 1.33 (ethyl acetate/toluene: 50/50), and 1.41 (toluene), respectively. Linear correlations were obtained between the MWCO and the swelling ratio induced by each solvent and between the MWCO and the transmembrane pressure. Pore size calculations using solvent flux and retention data confirmed the variable sieving properties of the PDMS membrane in relation to the solvent-induced swelling and applied transmembrane pressure. In addition, the study of the solute-transfer rate through several operating conditions showed that both diffusive and convective transports occurred for the PEG solutes and that their respective contributions appeared dependent on the variable pore size of the PDMS membrane. © 2014 Wiley Periodicals, Inc. J. Appl. Polym. Sci. **2014**, *131*, 41171.

KEYWORDS: elastomers; membranes; separation techniques; swelling

Received 26 July 2013; accepted 13 June 2014
DOI: 10.1002/app.41171

INTRODUCTION

Over the last few decades, solvent-resistant nanofiltration (SRNF) has been of great interest for study because of its several influential applications in separation processes involving organic solvents. Indeed, SRNF could be an environmentally friendly and economic means for replacing energy-consuming systems. Catalyst recovery, molecular sieving, chemical cracking, and the purification of active components constitute a nonexhaustive list of applications that could be considered taking into account current industrial and environmental requirements.[1]

The mechanisms of aqueous nanofiltration (NF) are fairly well documented but uncertainties remain about this process when organic solvents are used.[2] This is mainly owing to additional solvent–solute–membrane interactions.[3–9] Many studies have attempted to model mass transfer through such membranes. Bhanushali et al.[10] showed how both diffusion and convection contribute to solute transport (dyes and triacylglycerols). Furthermore, several studies[11–14] have shown that the balance between convective and diffusive transports would be mainly directed toward convective transport, especially when the solute size is much lower than the volume depicted by the interchain spaces in a polymer matrix. Zeidler et al.[15] showed that solute transfer through the membrane can be described using either the solution-diffusion model or the pore flow model, depending on the affinity between functional groups of the solute and the membrane. Given the variability in valid available models which can be used to describe solute transport through SRNF membranes, further investigations are needed to better understand the SRNF process and predict its performances.

In addition, rubbery polymers—among which poly(dimethylsiloxane) (PDMS) is well covered by the SRNF studies—exhibit certain properties which make it possible to envisage a selectivity-controlled NF process. The morphologic changes induced in the polymeric membrane by several operating parameters appear to play a major role. Unfortunately, the polymer structure depends on several operating conditions and this increased the complexity of characterizing both transport mechanisms and process performances. Difficulties in predicting this

kind of solvent-dependent behavior in membranes[16–19] have meant that the impact of operating parameters on the polymer network structure and on consequent sieving performances remains unclear.[20–23]

First, the swelling of a PDMS membrane is known to be dependent on the solvent that is put in contact with. In addition, for a given solvent, the amount of sorbed liquid in the polymer and concomitant increase of the interchain distances were reported to be strongly dependent on PDMS synthesis conditions—the initial amount of crosslinker,[24] vulcanization,[25] or plasma treatment,[26] addition of fillers such as silicates,[27] or metal organic framework[28] constitute a nonexhaustive list of treatments that induce different polymer layouts and crosslink densities. These criteria are known to have significant impact on the swelling capacity, mechanical properties, and permeation performances.

Second, when a thin PDMS film is used as an active layer in a SRNF experiment, it is subjected to two opposite influences. As described above, solvent-induced swelling tends to increase permeability and decrease retention.[29–32] Also, the film is exposed to significantly high transmembrane pressure (TMP) (usually, 20–40 bar) which would tend to flatten the swollen PDMS. Tarleton et al.[33] developed a specific apparatus to measure the swelling ratio of PDMS polymers under pressure. They noted that an applied pressure of 20 bar led to an 80% reduction of heptane-induced swelling as compared to the value obtained at atmospheric pressure. Similarly, Ogieglo et al.[34] noticed a significant reduction of the membrane's thickness induced by the applied TMP during NF experiments.

Finally, temperature has been found to strongly influence PDMS behavior when swollen with a solvent and/or submitted to compression strains.[35,36] Indeed, increased relaxation of the polymer chains as a consequence of the temperature increase leads to increased swelling of the polymer because of reduced limitations on the elastic forces. The polymer matrix is consequently softened which thus makes it more susceptible to compaction.

In this study, we attempted to better understand the relationship between the layout of a commercial PDMS membrane (depending on the operating conditions of the SRNF experiments) and its molecular sieving properties. Retention experiments were carried out using the homologous series of polyethylene glycols (PEGs, 200–1500 g mol^{-1}) to characterize the influences of swelling, TMP, and temperature on the solute retention.

MATERIALS AND METHODS

Membrane and Chemicals

This study was performed with commercially available dense PDMS membranes to overcome possible interferences related to the use of composite membranes and above all, because of the possibility of polymer intrusion into the support material which may have restricted PDMS swelling and performances.[37,38] This material was also expected to be highly reproducible and the supplier specifications suggested that it could be obtained by exactly the same synthesis process for all studied thicknesses. The membrane used throughout the study was a dense 125-μm thick PDMS film purchased from ETHICON (Issy les Moulineaux, France). Flat sheet samples of PDMS with a 1.5 mm of thickness (same provider) were also used for measuring swelling. The solvents used for swelling experiments and for formulating the feed mixtures for the NF investigations were toluene, ethyl acetate, and ethanol—all from Sigma Aldrich® (Saint Quentin Fallavier, France) and all are of analytical grade. The PEG solutes were obtained from the same supplier. Their molar masses were 200, 400, 600, 1000, and 1500 g mol^{-1}, respectively.

NF Experiments

The four solvents or mixtures used throughout this study were selected from a previous study of the swelling and compressibility of the PDMS membrane.[39] They presented linear relationships ($R^2 > 0.99$) between:

1. The values of the Hildebrand solubility parameter (HSP) and the proportion of solvent in the PDMS/solvent system (φ_S).
2. The solvent volume in the membrane and the total volume of the PDMS/solvent system.
3. The molar mass (calculated with the Phantom model) between the polymer chains and the swelling ratios.
4. For mixtures, the measured swelling ratio (S_L, the ratio of the dimensions of a swollen PDMS sample to the dimensions of the same sample in its dry state) and the molar contribution of each solvent to this value.
5. The TMP and the corrected solvent fluxes that take into account both swelling and compressibility of the PDMS membrane.

These criteria appeared of great importance for a study of retention performances, and hence avoiding any unexpected effects of solvent–membrane interactions (e.g., swelling extent as a function of affinity for the membrane, high fluxes despite a weak swelling, strong retentionship whereas the swelling degree is high, etc.) as much as possible. Thus, it was expected that the performances could be predicted from just a small amount of experimental data to extrapolate to the entire range of the assessed operating conditions. The four selected solvents are listed in Table I along with their main properties which influence the NF process.

The NF device was composed of a laboratory-made tangential device with an effective filtration area of 30 cm^2 and equipped with a pressure gauge (Figure 1). The filtration module consisted of two stainless steel rings, ensuring membrane maintenance and tightness, a stainless steel macroporous mechanical support and a protection paper between the PDMS membrane and this support. The module was fed with an high-performance liquid chromatography pump and a pressure control valve allowed TMP regulation from 1 to 50 bar. The permeate was collected and its weight recorded using precision scales (*Sartorius*®) through an acquisition software (Testpoint®).

Before it was put in the module, the PDMS membrane was systematically swollen in the solvent used for the subsequent

Table I. Main Properties of the Solvents Selected for the Retention Study

	Solvents			
Main properties	Ethyl acetate/ethanol (25/75)	Ethyl acetate	Ethyl acetate/toluene (25/75)	Toluene
Molar volume (cm^3 mol^{-1})	85.39	98.23	102.40	106.04
Viscosity (25°C, mPa s)	0.47	0.43	0.52	0.59
Density (g cm^{-3})	0.86	0.92	0.88	0.87
HSP values ($MPa^{1/2}$)	20.80	18.60	18.40	18.20
S_L (25°C, P_{atm})	1.16	1.26	1.33	1.41
φ_S (cm^3 cm^{-3} swollen polymer)	0.41	0.53	0.55	0.57
Permeability[a] (L h^{-1} m^{-2})	1.60	4.44	5.78	6.55
Solute diffusivity (10^{-7} m^2 s^{-1})				
PEG 200	1.69	2.38	1.86	1.55
PEG 400	1.07	1.50	1.18	0.98
PEG 600	0.86	1.22	0.95	0.79
PEG 1000	0.63	0.89	0.70	0.58

[a] The indicated permeability values were obtained under the standard conditions explained in the **Materials and Methods** section. Solvent proportions in the mixtures are expressed as volume percentage (vol : vol).

permeation experiment to ensure that volume expansion caused by solvent uptake did not affect the area and shape of the filtration layer. For each solvent, at least two membranes were tested with three measurements of fluxes at each pressure level. A steady state of permeation was usually reached after 10 min and was checked by the linearity of the relationship between recorded permeate weight and filtration duration. All the experiments were performed using a feed rate of 5 mL min^{-1}. Finally, the permeate flux through the membrane was calculated using the following equation:

$$J = \frac{m}{\rho A t} \quad (1)$$

J is the permeate flux (L h^{-1} m^{-2}), m the permeate mass (g), ρ the solvent density (g L^{-1}), A the membrane area (m^2), and t the permeation duration (h).

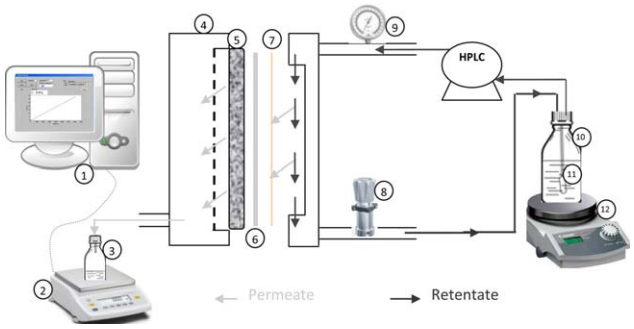

Figure 1. The NF device: 1, acquisition computer; 2, precision balance; 3, collected permeate; 4, stainless steel ring; 5, stainless steel macroporous support; 6, protection macroporous paper; 7, swollen PDMS membrane; 8, pressure control valve; 9, pressure gauge; 10, feed solution/retentate; 11, helium sparger; and 12, magnetic stirring controller. [Color figure can be viewed in the online issue, which is available at wileyonlinelibrary.com.]

Retention Assessments for Molecular Weight Cutoff Estimation

The same tangential filtration module and PDMS membrane were used to study the retention of the homologous series of uncharged solutes (200, 400, 600, and 1000 g mol^{-1} PEGs). The standard operating condition was a 200 mL feed solution of toluene ($S_L = 1.41$) with a solute concentration of 5 gL^{-1} which was filtered under 30-bar TMP until a volume concentration factor (VCF) of 2 was reached and at 25°C and 5 mL min^{-1} of feed rate. To study the parameters' impact on retention values, each of them was varied by maintaining the others at their standard level. The assessed ranges were, respectively, 1.16–1.41 for S_L, 10–32.5°C for the operating temperature, 5–50 bar for the TMP, and 2–8 for the VCF. The resulting concentrations of PEGs in permeate (C_p) and retentate (C_R) were determined by gravimetric measurement and checked using a chromatographic analysis. The device (LC 20A, Shimadzu®) was equipped with a Superdex peptide GE® column and an evaporative light scattering detector (ELSD-LT II, Shimadzu®). The size exclusion column allowed for a tight size distribution of the PEGs to be confirmed. All concentrations were determined from external calibration curves. Each measurement was repeated three times. Standard deviations were <1.5%. The resulting retention (R) and solute fluxes (J_S in g h^{-1} m^{-2}) were calculated as follows:

$$R = 1 - \frac{C_P}{C_R} \quad (2)$$

$$J_S = C_P J \quad (3)$$

The mass acquisition software enabled to precisely record the amount of solution crossing the PDMS membrane during the filtration experiments. Between each experiment on the PEG solutes, the system was thoroughly flushed with the solvent used for the retention experiments ("flushing" step). Recovery of the initial solvent flux was checked before any subsequent filtration.

Table II. Reproducibility Evaluation of the Retention Values for Two PEG Solutes (200 and 1000 g mol^{-1})

Experiments	R_{PEG200} (%)	$R_{PEG1000}$ (%)
M_1 exp. 1	56.01	95.97
M_1 exp. 2	56.63	96.09
M_1 exp. 3	55.90	96.36
M_1 exp. 4	56.14	95.89
SD M_1 exps. 1–4	**0.32**	**0.20**
M_2 exp. 1	58.52	96.79
M_2 exp. 2	57.86	97.02
SD M_1/M_2	**1.43**	**0.59**
Global SD	**1.09**	**0.46**

By definition, the molecular weight cutoff (MWCO) (g mol^{-1}) corresponds to the molecular weight of a solute for which the retention value reaches 0.9. In this study, the MWCO values of the PDMS membrane under different experimental conditions were deduced from the curves, depicting the PEG's retention as a function of their molecular weight.

Pore Size Calculation

To confirm the changes in the PDMS structure induced by variable operating conditions, pore size calculations were carried out both from solvent fluxes (published in an earlier study[39]) and from retention data. For the first set of experimental results, the Hagen–Poiseuille equation was used, approximating the polymer interchain's volume to straight cylindrical pores.[40] Thus, the mean "pore" size was obtained with the correlation:

$$r_p = \sqrt{\frac{J 8 \mu L}{\mathrm{TMP}\varepsilon}} \tag{4}$$

where r_p is the mean pore radius (m), J the solvent flux ($m^3\ s^{-1}\ m^{-2}$), μ the dynamic viscosity of the solvent (Pa s), L the membrane thickness (m), varying with the TMP according to the previous compression study,[39] TMP the TMP (Pa), and ε the porosity considered here as the solvent volume fraction contained in the swollen PDMS polymer for each couple of swelling ratios and applied pressures.

The r_P values calculated from retention values were obtained by using the extended pore-flow model (PFM) extensively described in scientific literature on this subject.[41–44] The solute transfer is considered as a result from both convection and diffusion through the pores. The contributions made by each driving force to solute transfer are particularly influenced by the steric hindrance of the solute and the rheological properties of the fluid they are dissolved in. The solute rejection is expressed as:

$$R = 1 - \frac{K_c \Phi}{1 - \exp(-\mathrm{Pe})[1 - \Phi K_c]} \tag{5}$$

Φ is a steric term relating the size of the solute and pore size:

$$\Phi = (1-\lambda)^2 \tag{6}$$

where λ is the ratio of solute to pore size. Pe is the Peclet number defined as:

$$\mathrm{Pe} = \frac{K_c}{K_d D}\frac{r_p \mathrm{TMP}}{8\mu} \tag{7}$$

D is the solute diffusivity ($m^2\ s^{-1}$). K_c and K_d are the hindrance factors for the convection and the diffusion, respectively. Assuming a homogeneous velocity for transport of solute through the PDMS membrane (very small pore radii), the two hindrance factors for uncharged solutes can be computed from the lambda ratio as[45]:

$$K_d = 1 - 2.30\lambda + 1.15\lambda^2 + 0.22\lambda^3 \tag{8}$$

$$K_c = (2-\Phi)(1 + 0.05\lambda - 0.99\lambda^2 + 0.44\lambda^3) \tag{9}$$

To allow for the calculation of the pore radii employing the PFM model, the PEG radii (r_S) was calculated with the Stokes–Einstein equation[46]:

$$r_S = \frac{k_B T}{6\pi\mu D} \tag{10}$$

with k_B the Boltzmann constant and T the temperature (K). It is interesting to note that the experiments of sorption for pure PEG solutions were carried out and that neither swelling nor sorption was measured for these solutes. In view of this result, it was assumed that the only way for PEG solute to diffuse through the membrane was by diffusion through the solvent filling the interchain volume of the polymer. The Wilke–Chang equation was therefore considered valid to estimate the PEG diffusivity in this study and thus the solute diffusivity (D in $m^2\ s^{-1}$) through the membrane was calculated using the Wilke–Chang equation[47] as follows:

$$D = 7.4\times10^{-8} \times \frac{T\sqrt{\alpha M}}{\mu {V_m}^{0.6}} \tag{11}$$

where M is the solvent molar mass (kg mol^{-1}), V_m the molar volume of the solute ($m^3\ mol^{-1}$) estimated using a group contribution method.[48] Finally, the mean pore radii were estimated by making eq. (5) match with the experimental retention values.

EXPERIMENTAL

Filtration Through the PDMS: Reproducibility and Flux Performances

First of all, the reproducibility of the sieving properties was evaluated to confirm the similarity between the different PDMS sheets used throughout the study. Filtrations were performed with intermediate flushing (permeation of the solvent or solvent/solvent mixture used for the retention experiments without any solute) to evaluate the permeation reproducibility with the two solutes having the extreme values of solute sizes (200 and 1000 g mol^{-1}). The results are summarized in Table II.

Experimental errors caused by the precision levels of the apparatus used for flux and retention determinations were responsible 5.3 × 10^{-3} fluctuation retention values at the most. For the same membrane ($M1$), reproducibility was comparatively very good with the deviation (3 and 2 × 10^{-3} units of retention for PEG200 and PEG1000, respectively) found to be inferior for possible experimental error. Experiments which included retention assessments and subsequent flushings (total duration of 20 h of filtration with the same membrane sample) showed an

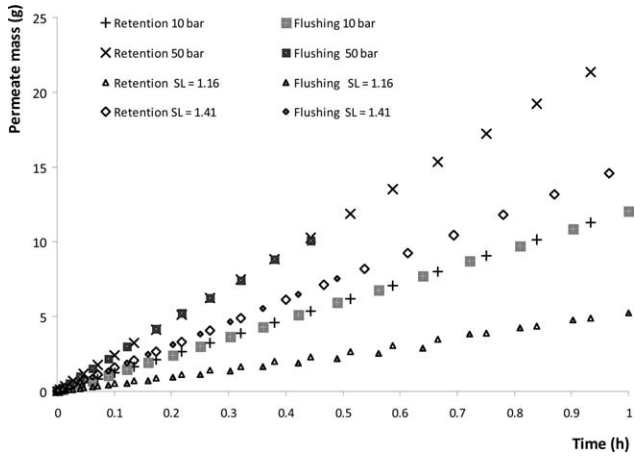

Figure 2. Mass acquisition during the NF experiments, with (retention) or without (subsequent flushing) solute (PEG, 200 g mol^{-1}) in the feed solution, under different experimental conditions.

appreciable stability of the sieving properties of the PDMS membrane. In contrast, higher deviations were observed between two different membrane pieces (*M*1 and *M*2) and these were obviously more pronounced for the weakest solute size as a significantly larger amount of it permeated through the membrane. The fluctuations observed between two different PDMS membranes were attributed to the inherent and intrinsic properties of the PDMS polymer (variable distribution of crosslinks during the polymerization, polymer defects, and variable entanglements of the polymer chains, etc.). Nevertheless, any fluctuations remained sufficiently weak compared to the value of retention. To improve the accuracy of the retention measurements, the experiences were carried out as long as possible on the same membrane sheet.

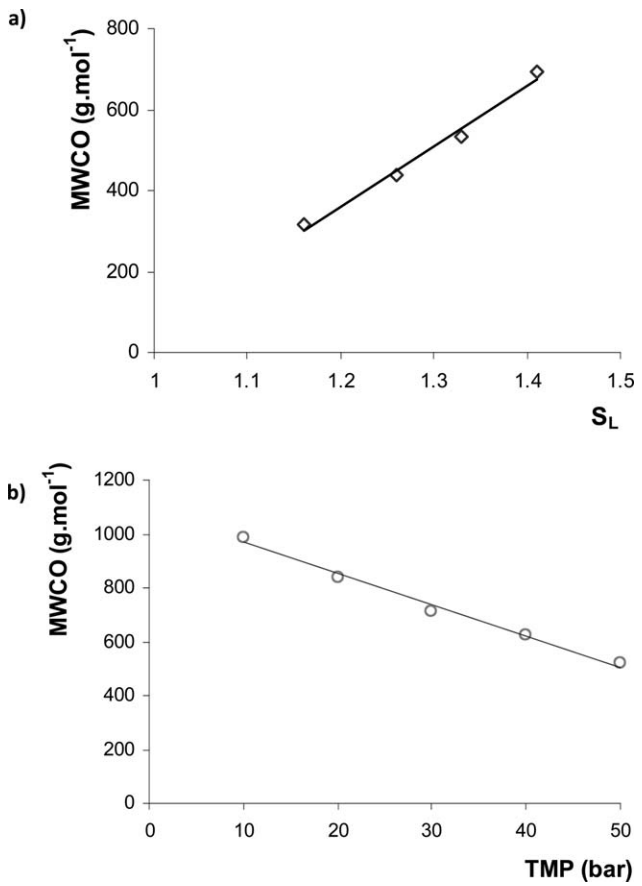

Figure 3. MWCOs of the PDMS membrane as a function of the swelling ratio (a) and the TMP (b).

In addition, the influence of the presence of a solute in the feed solution on the overall permeation rate was evaluated through several experimental parameters. The corresponding permeation fluxes without (flushing) and with the PEG200 solute (retention) are shown in Figure 2.

The fluxes were found to be strictly similar with or without a solute for each operating condition and thus showing that the presence of solute had a negligible influence on the overall permeation rate. Thus, it was assumed that no fouling occurred during the filtration experiments, that the concentration polarization was negligible and that the hydrodynamic properties of the solutions permeating were not affected to any significant extent by the presence of solutes at an initial concentration of 5 g L^{-1}.

Sieving Performance in Relation to the Operating Conditions of the NF

Influence of Swelling and TMP on MWCO and Pore Size. The MWCO is often considered to characterize the rejection properties of a membrane. In the case of uncharged molecules, the solute molecular weight inducing a rejection value of 90% may indeed provide an accurate description of the membrane's sieving properties. However, in SRNF, the MWCO appeared to be solvent dependent.[8,28,41] Until now, it had not been possible to obtain any rigorous relationships between the solvent-induced swelling and the MWCO. To demonstrate the key role of the extent of swelling, TMP and temperature in defining the PDMS membrane's sieving properties, the retentions of the homologous series of PEGs were measured under various operating conditions (solvent, TMP, and temperature). The resulting MWCOs are shown in Figure 3.

As shown in Figure 3(a), the MWCO of the PDMS membrane plotted as a function of the swelling ratio gives a linear relationship. The MWCO increased from 315 to 685 g mol^{-1} for S_L values between 1.16 and 1.41, respectively. The MWCO in relation to the TMP [Figure 3(b)] also shows a linear relationship, characterized by an inverse variation. Indeed, the MWCO values were found to range from 519 g mol^{-1} at 50 bar to 689 g mol^{-1} at 10 bar. Although they were obtained under the same experimental conditions, there was a slight difference between the values of MWCOs at $S_L = 1.41$ [Figure 3(a)] and the value at 30 bar applied pressure [Figure 3(b)]. This 25 g mol^{-1} discrepancy (MWCO of 685 and 710 g mol^{-1}, respectively) was attributed to the variability between two different PDMS membranes (experiments for the evaluation of the swelling impact and the TMP influence were carried out with two different PDMS films) and also to the deviation resulting from both analytical measurements and graphical determinations of the MWCO.

To evaluate the accuracy of using the hydraulic theory to describe the permeation through PDMS membranes, the pore size was calculated from both pure solvent fluxes[39] and

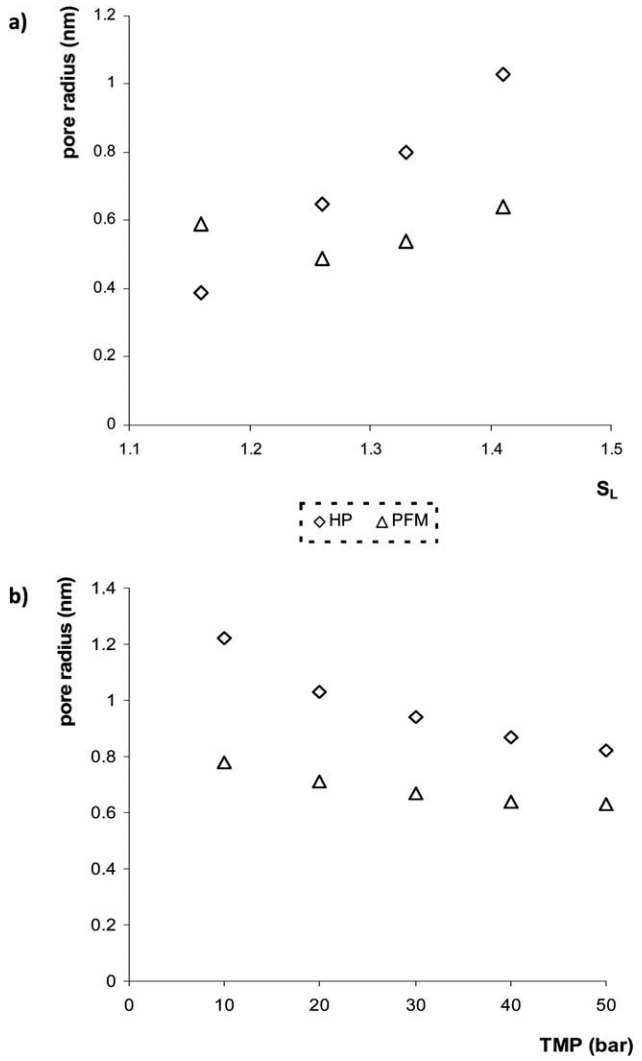

Figure 4. Evolution of the pore size as a function of: (a) the swelling degree (S_L) and (b) the TMP values. The calculation of the pore radii was carried out from the pure solvent fluxes employing the Hagen–Poiseuille model (HP) and from the PEG retention data using the PFM.

retention values. Two corresponding hydrodynamic models were used—the Hagen–Poiseuille model for the values of solvent fluxes and a revised pore flow model which allows for the calculation of the pore radius from retention data. The values of the pore radii obtained for each assessed operating parameters are shown in Figure 4.

Regardless of the model used, the pore sizes were found to be of the same order of magnitude as sizes reported in the literature[44,49] with only a few nanometers difference if any. The differences observed for the pore radii obtained through both models from two distinct pools of data (using either the values of solvent fluxes or the PEG retention results) may result from the roughness of the models (cylindrical pores, single diameter, etc.) and the use of correlations for hindrance factors' calculation (whereas the correlations used in this study gave the best adequacy between the two models among the numerous correlations that are available, they were not initially deduced from PEG retention studies[45]).

Nevertheless, the evolution of the pore radii with the swelling degree explains at least in part the evolution of the MWCOs [Figure 4(a)]. Similarly to the MWCO, the pore radius calculated through the Hagen–Poiseuille model presented a linear increase with the S_L values ($R^2 > 0.99$; data not shown). This increase reflects the variable distances between crosslinks which are known to be dependent on the swelling state of the PDMS. The PFM was found to show an inconsistency in pore size calculated for the weakest swelling degree (ethanol/ethyl acetate mixture, $S_L = 1.16$). This value had a pore radius superior to those obtained for some higher swelling degrees which does indeed deviate significantly from the linear relationship between pore radii and swelling degrees obtained for the other solvents. As an accurate value at $S_L = 1.16$ was obtained when the pore radius was calculated from the solvent fluxes (Hagen–Poiseuille model) and in view of the evolution of the MWCO as a function of the S_L values, this unexpected upper trend could be interpreted as showing that the PFM does not adequately estimate the pore size for the ethanol/ethyl acetate mixture. In addition to the previously mentioned roughness of the PFM model and use of available correlations for the hindrance factors, one additional reason for this kind of result could be inaccurate estimation of the diffusivity of the solutes calculated using the Wilke–Chang equation. More precisely, the solvent parameter (α), equals to 1 for pure solvents, may differ significantly from unity for the ethanol/ethyl acetate mixture and thus affect estimations for both D and r_S values. Unfortunately, a more accurate value for this solvent mixture cannot be found in available data on this subject.

Concerning the evolution of the pore radii in relation to the TMP [Figure 4(b)], both models presented similar trends which depict the behavior of the swollen PDMS when submitted to compression (dual poro- and viscoelastic behavior)[39] namely a large decrease under moderate amounts of applied pressure (TMP < 20–25 bar) and a weaker influence at TMP values over this threshold, with a relationship between the pore radius and the TMP tending toward the linear.

Influence of the Operating Temperature. First, to evaluate the extent to which swelling levels could have influenced retention results and the mechanism involved in this, the swelling of the PDMS membrane was measured by length (S_L) and weight (S_W) increases within a broad range of temperatures. Both measurements were assessed according to the method presented in a previous study.[39] The length increase shows the total volumetric expansion of the polymer soaked in solvent and the weight increase is attributed to the amount of sorbed solvent in the PDMS. The swelling levels obtained are shown in Figure 5(a). S_L and S_W values were found to increase with temperature, ranging from 1.40 and 2.19 at 8°C to 1.46 and 2.39 at 42°C, respectively. It is worth noting at this point that the two swelling degrees evolved in the same manner and thus confirming the idea that the relaxation of the constitutive chains of the PDMS polymer and the amount of sorbed solvent are strictly related (filling the interchain volume by the solvent molecules).

Second, the MWCO values were deduced from the PEG retention curves and are shown in Figure 5(b). Their values vary in

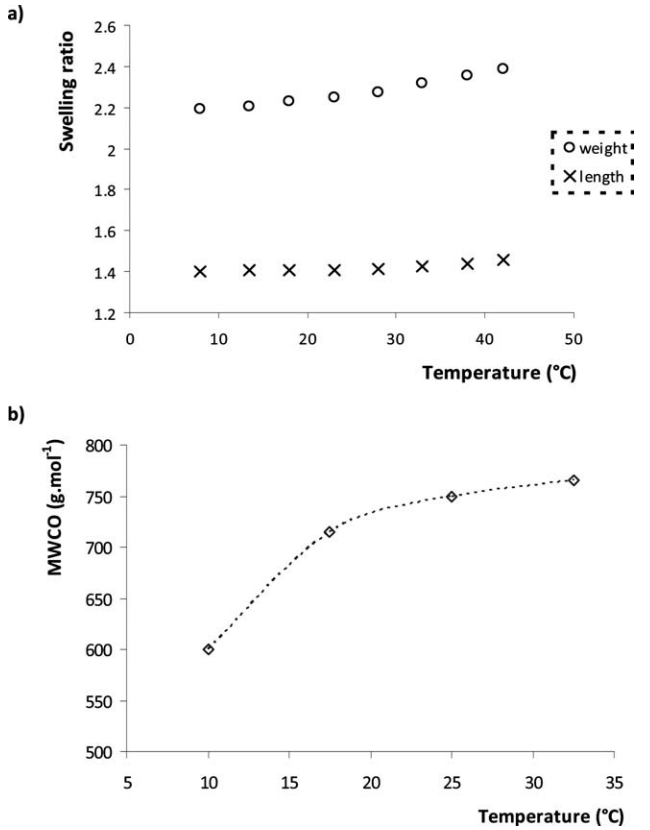

Figure 5. Evolution of the swelling degree (a) and the MWCO (b) as a function of the operating temperature.

the same way as the temperature. A rise from 10 to 37.5°C was found to increase the MWCO values from 600 to 765 g mol^{-1}. However, the relationship did not appear to be linear in this case—the increase in the MWCO was more pronounced between 10 and 20°C than after this temperature threshold. Unfortunately, the pore size calculation could be carried out because the experimental device used for PDMS compressibility measurements cannot be thermoregulated and thus data on the evolution of the viscosity values in correlation with temperature for the solvent mixtures used throughout this study are not available.

Solute-Transfer Rates. To help understand more about the transport mechanisms involved in solute transfer through the PDMS membrane and the role of variable PDMS layouts in relation to the operating conditions of the NF process, the solute fluxes (J_S) were calculated according to eq. (3). The results obtained for all the experiments are shown in Figure 6.

The three profiles of the evolution of J_S were found to be strictly different for each of the operating parameters assessed. Regardless of the solute size, the transfer rates were found to increase exponentially with the level of swelling [Figure 6(a)]. In contrast, a size-dependent evolution of solute transfer was evident regarding the impact of the TMP [Figure 6(b)]. Indeed, although its rate was found to increase with the TMP for the smallest PEG, showing a logarithmic shape of the curve, the value of J_S for the largest solute decreased when the amount of pressure applied increased. In addition, the two other solutes displayed intermediate behavior, with a maximal transfer rate reached at different TMP values above which the transfer rate was seen to diminish. The shapes of the curves are similar as far as temperature is concerned [Figure 6(c)] for all PEG sizes. Two

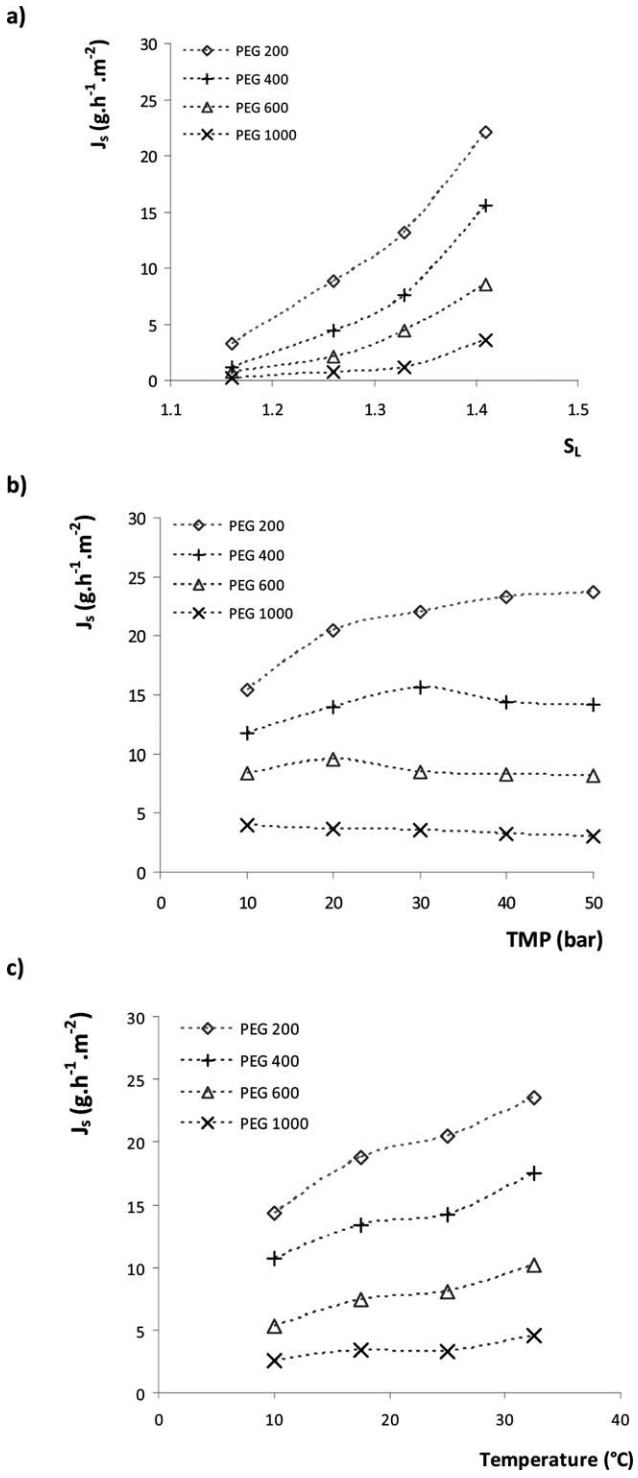

Figure 6. Solute-transfer rates in relation to the swelling degree (a), the TMP (b), and the operating temperature (c) for a homologous series of PEGs (200, 400, 600, and 1000 g mol^{-1}) dissolved in toluene.

phases of increase with the operating temperature can be highlighted. The first has a logarithmic profile (10–25°C), whereas the second ($T > 25$°C), presents an exponential increase of the transfer rate.

DISCUSSION

Influence of Swelling on the PDMS Sieving Properties

Basically, the swelling of the PDMS polymer leads to simultaneous morphologic and physicochemical changes which influence its sieving properties mainly through the following factors: an increase in the distances between crosslinks in the polymer (enhanced access for the solute into the membrane at the solution/membrane interface, facilitated crossing of the solute through the polymer), opening of polymer chain entanglements (new connected pores), an increase of the membrane thickness, an enhanced permeation velocity (friction forces), and a filling of the interchain volume by the solvent that sorbs into the PDMS.[29–34,39,50] The linearity of the MWCOs in relation to the S_L values [Figure 3(a)] shows that the solvent-induced increase of the interchain distances in the polymer appears to be a main parameter governing solute rejection. The pore size calculation through the hydraulic theory of transport was consistent overall with the evolution of the PDMS membrane's sieving properties. A linear increase to the pore radii with the S_L values [Figure 4(a)] corroborates the theory that membrane pores opening is proportional to the degree of swelling.

An interesting point can also be made regarding the solute-transfer rate as a function of the swelling degree [Figure 6(a)]—the minor effects of the increase in membrane thickness and the enhancement of permeation velocity with S_L, which are both known to slow down solute permeation. In view of the exponential increase of the PEGs' transfer rate with S_L, their impact may be counterbalanced by:

i. New connecting "pores" opening which are dependent on the extent of swelling. Indeed, swelling of the PDMS was shown to considerably reduce the contribution of entanglements to overall crosslink density.[18]
ii. Differences in thickness of membranes at various S_L values which are minimized owing to TMP-induced compressibility of the PDMS (TMP = 30 bar).[39]
iii. Friction forces which are softened more by the increase of pore size than they are enhanced by the increase in permeation velocity.

The different values of solute diffusivities (Table I) were not reflected in the results of PEG transfer (exponential increase of transfer rate whereas the diffusivity of PEGs decreases in the solvent inducing S_L from 1.26 to 1.41). This finding could be explained by transport mainly governed by convection forces.

Influence of the TMP on the PEG Permeation

Concerning the effect of the TMP on the solute retention, the rejection increases with the TMP values. This result may be a consequence of several mechanisms namely reduction of the solvent proportion in the polymer and decrease of the interchain distances (less swelling and pressure-induced compaction) or increase of the overall permeation velocity (increased friction forces). These impacts of TMP on the PDMS structure were confirmed by the evolution of the MWCOs and the calculated pore radii [Figures 3(b) and 4(b)].

In addition, the evolution of the permeation rate of the solutes according to the pressure applied appears size dependent [Figure 6(b)]. For each solute size, the maximal transfer rate was reached at a different TMP value. Although for the 200 g mol^{-1} PEG, the maximal rate was achieved at 50 bar, the TMP value at which the maximal rate of permeation was reached for the other solutes decreased when their molecular weight increased. Two main correlated reasons may be responsible for the observed J_S profiles:

i. A balance between forces enhancing or weakening solute permeation. Indeed, although an elevation in TMP values leads to an increase in the driving force through the membrane and a reduction in the membrane thickness (increase of the transfer rate), the TMP increase also results in reduced membrane swelling which restricts access to the membrane and slows down solute permeation through the PDMS membrane. Both diffusive and convective transport would be affected, the former mainly by a reduced proportion of solvent in the PDMS through which the solute diffuses and the latter by narrower pore sizes induced by the TMP increase. In addition, the increase of friction forces with the TMP-enhanced overall permeation velocity can be viewed as an additional mechanism which leads to a reduction in solute-transfer rates in relation with the TMP.
ii. The variable contribution of convective and diffusive transport to the value of J_S. It is well known that the balance between convective and diffusive transports is conditioned by the difference between pore size and solute diameter.[50] In the case of PDMS, the greater the TMP value and solute sizes, the lower this difference will be. Hence, for small solutes (case of the 200 g mol^{-1} PEG), we may suppose that the size difference between the solute molecule and the interchain spaces would have remained significantly important in the entire range of TMP values. The logarithmic trend of J_S [Figure 6(b)], also observed for pure solvent fluxes,[39] would thus underline a high convective flux which accounts for the predominant part of the total solute flux. For medium solute sizes (PEG, 400 and 600 g mol^{-1}), the same assumption can be made but only up to a threshold value of TMP at which the pore size becomes equivalent to the size of the solute molecule. Beyond this threshold value, the convective flux would become negligible. The subsequent decrease of J_S values may imply transport predominately governed by diffusion through the solvent contained in the PDMS membrane. The latter solute transfer would then be the only mechanism involved in the permeation of the largest PEG solute (1000 g mol^{-1}). The decrease of its J_S value from 10 to 50 bar can mainly be explained by the decrease in the solvent proportion into the PDMS membrane along this TMP elevation.

Finally, current controversy within SRNF community about the extent of impact of swelling and TMP and the debate about transport mechanisms involved in solute transfer are legitimate

subjects for discussion but both can be explained by the experimental setup chosen in the different studies carried out (nature and thickness of PDMS, range of pressures applied, solute size, etc.).

Effects of Temperature on the NF Process

The temperature at which the NF experiment is carried out has multiple and various impact on the NF process. Thus, the increase of the MWCO with higher temperatures may result from:

1. Hydrodynamic consideration: the decrease in solvent viscosity at higher temperatures contributes to the enhancement of the overall permeation rate and the diffusivity of the PEG solute in the solvent according to the Wilke–Chang equation (eq. 6).[35,46]
2. Molecular reactivity: sorption of the solvent into the membrane and consequent membrane swelling,[51] molecular motion, and flexibility.[15]
3. Physical considerations: polymer stiffness (sensitivity to compaction).[18]

The increase in swelling with rising temperatures [Figure 5(a)] in correlation with the MWCO increase confirms the importance of the PDMS layout for solute permeation. Its predominance compared to the impact of friction forces induced by an increase of the flux velocity appears obvious. Indeed, although the overall permeation rate (mainly attributed to the solvent permeation) decreases when the operating temperature is diminished, the PEG retention increases significantly. This increase, being concomitant to the decrease of the S_L value, corroborates the theory of a sieving mechanism which strongly depends on the extent of polymer swelling. At low temperatures, a reduced solvent proportion in the membrane and the shortened molecule paths (as a consequence of less solvent-induced distances between the polymer chains) might play a major role in increasing retention [Figure 5(b)]. Nevertheless, the evolution of solvent-dependent swelling and MWCO values did not follow the same trend in the temperature range studied. Indeed, in view of the evolution of swelling dependence to temperature, the exclusive impact of temperature does not provide a satisfying explanation, given the temperature-dependent transfer rate of the solute [Figure 6(c)]. The latter may be a consequence of a balance between the various properties of the NF system affected by the temperature. Finally, the mechanisms involved in the temperature dependence of the solute transfer appeared to be a consequence of several molecular and structural properties. It is difficult to completely understand these mechanisms because of the complexity of the system and possible synergistic effects. Nevertheless, with an appropriate membrane calibration method, this operating parameter appears useful to selectively modify the performances of the NF process with PDMS membranes.

CONCLUSIONS

This study aimed to clarify the impact of the PDMS structure on its permeation properties. Three selected solvents were used, pure or as mixtures, to perform NF experiments with the homologous series of PEGs at different swelling degrees, TMPs, and temperatures. The results of the corresponding MWCO values and/or solute-transfer rates provided significant insight into the PDMS permeation properties. The swelling induced by the solvents ($S_L = 1.16–1.41$) and the amount of applied pressure (TMP = 10–50 bar) appeared to be linearly correlated to the MWCO of the PDMS membrane. The calculation of pore size based on the hydrodynamic theory was consistent with the measured MWCOs. Increase of the pore size with swelling and its decrease as a consequence of TMP elevation corroborated the polymer properties when immersed in a solvent and submitted to compression. Obviously, the probabilities for solutes to gain access to the membrane as well as the transport throughout the PDMS layer are governed by the membrane's condition-dependent structure. Temperature was found to be a useful additional parameter to modify the permeation properties of the PDMS membrane and to impact both membrane and hydrodynamic properties. The study of the transfer rate of the PEG solutes confirmed a dual convective/diffusive transport involved in the solute permeation among which contributions are conditioned by the difference between the interchain distances and the molecular weight of the solute. All the results obtained confirmed that the control of the PDMS structure is a potent tool for varying its permeation properties. Depending on the swelling extent, the pressure applied and temperature, the membrane pore size can be selectively modified by an appropriate choice of operating parameters.

REFERENCES

1. Volkov, A. V.; Korneeva, G. A. Tereshchenko, G. F. *Russian Chem. Rev.* **2008**, *77*, 983.
2. Vandezande, P.; Gevers, L. E. M.; Vankelecom, I. F. J. *Chem. Soc. Rev.* **2008**, *37*, 365.
3. Bhanushali, D.; Kloos, S.; Kurth, C.; Bhattacharyya, D. *J. Membr. Sci.* **2001**, *189*, 1.
4. Vankelecom, I. F. J.; de Smet, K.; Gevers, L. E. M.; Livingston, A.; Nair, D.; Aerts, S.; Kuypers. S.; Jacobs, P. A. *J. Membr. Sci.* **2004**, *231*, 99.
5. Robinson, J. P.; Tarleton, E. S.; Millington, C. R.; Nijmeijer, A. *J. Membr. Sci.* **2004**, *230*, 29.
6. Darvishmanesh, S.; Degreve, J.; Van der Bruggen, B. *Chem. Eng. Sci.* **2009**, *64*, 3914.
7. Machado, D. R.; Hasson, D.; Semiat, R. *J. Membr. Sci.* **1999**, *163*, 93.
8. Yang, X. J.; Livingston, A. G.; Freitas dos Santos, L. *J. Membr. Sci.* **2001**, *190*, 45.
9. Darvishmanesh, S.; Buekenhoudt, A.; Degrève, J.; Van der Bruggen, B. *J. Membr. Sci.* **2009**, *334*, 43.
10. Bhanushali, D.; Kloos, S.; Bhattacharyya, D. *J. Membr. Sci.* **2002**, *208*, 343.
11. Dias, M.; Hadgraft, J.; Lane, M. E. *Int. J. Pharm.* **2007**, *336*, 108.
12. Ahmad, A. L.; Ooi, B. S. *Sep. Purif. Technol.* **2006**, *50*, 300.

13. Bellona, C.; Drewes, J. E.; Xu, P.; Amy, G. *Water Res.* **2004**, *38*, 2795.
14. Santos, J. L. C.; de Beukelaar, P.; Vankelecom, I. F. J.; Velizarovand, S.; Crespo, J. G. *Sep. Purif. Technol.* **2006**, *50*, 122.
15. Zeidler, S.; Kätzel, U.; Kreis, P. *J. Membr. Sci.* **2013**, *429*, 295.
16. Lee, J. N.; Park, C.; Whitesides, G. M. *Anal. Chem.* **2003**, *75*, 6544.
17. Carillo, F.; Gupta, S.; Balooch, M.; Marshall, S. J.; Marshall, G. W.; Pruitt, L.; Puttlitz, C. M. *J. Mater. Res.* **2005**, *20*, 2820.
18. Yoo, S. H.; Cohen, C.; Hui, C.-Y. *Polymer* **2006**, *47*, 6226.
19. Lange, J. J.; Collinson, M. M.; Culbertson, C. T.; Higgins, D. A. *Anal. Chem.* **2009**, *81*, 10089.
20. Gibbins, E.; Antonio, M.; Nair, D.; White, L. S.; Freitas dos Santos, L. M.; Vankelecom, I. J. F.; Livingston, A. G. *Desalination* **2002**, *147*, 307.
21. Stamatialis, D. F.; Stafie, N.; Buadu, K.; Hempenius, M.; Wessling, M. *J. Membr. Sci.* **2006**, *279*, 424.
22. Zwijnenberg, H. J.; Dutczak, S. M.; Boerrigter, M. E.; Hempenius, M. A.; Luiten-Olieman, M. W. J.; Benes, N. E.; Wessling, M.; Stamatialis, D. *J. Membr. Sci.* **2012**, *390*, 211.
23. Ben Soltane, H.; Roizard, D.; Favre, E. *J. Membr. Sci* **2013**, *435*, 110.
24. Cohen-Addad, J. P.; Domard, M.; Lorentz, G. *J. Phys.* **1984**, *45*, 575.
25. Yoo, J. S.; Kim, S. J.; Choi, J. S. *J. Chem. Eng. Data* **1999**, *44*, 16.
26. Aerts, S.; Vanhulsel, A.; Buekenhoudt, A.; Weyten, H.; Kuypers, S.; Chen, H.; Bryjak, M.; Gevers, L. E. M.; Vankelecom, I. F. J.; Jacobs, P. A. *J. Membr. Sci.* **2006**, *275*, 212.
27. Dobrak-Van Berlo, A.; Vankelecom, I. F. J.; Van der Bruggen, B. *J. Membr. Sci.* **2011**, *374*, 138.
28. Basu, S.; Maes, M.; Cano-Odena, A.; Alaerts, L.; De Vos, D. E.; Vankelecom, I. F. J. *J. Membr. Sci.* **2009**, *344*, 190.
29. Gevers, L. E. M.; Vankelecom, I. J. F.; Jacobs, P. A. *J. Membr. Sci.* **2006**, *278*, 199.
30. Ebert, K.; Koll, J.; Djikstra, M. F. J.; Eggers, M. *J. Membr. Sci.* **2006**, *285*, 75.
31. Stafie, N.; Stamatialis, D. F.; Wessling, M. *J. Membr. Sci.* **2004**, *228*, 103.
32. Vankelecom, I. J. F.; Moermans, B.; Verschueren, G.; Jacobs, P. A. *J. Membr. Sci.* **1999**, *158*, 289.
33. Tarleton, E. S.; Robinson, J. P.; Smith, S. J.; Na, J. J. W. *J. Membr. Sci.* **2005**, *261*, 129.
34. Ogieglo, W.; van der Werf, H.; Tempelman, K.; Wormeester, H.; Wessling, M.; Nijmeijer, A.; Benes, N. E. *J. Membr. Sci.* **2013**, *431*, 233.
35. Hooper, J. B.; Bedrov, D.; Smith, G. D.; Hanson, B.; Borodin, O. *J. Chem. Phys.* **2009**, *130*, 144904.
36. Pandey, S.; Rath, S. K.; Samui, A. B. *Ind. Eng. Chem. Res.* **2012**, *51*, 3531.
37. Dutczak, S. M.; Luiten-Olieman, M. W. J.; Zwinjnenberg, H. J.; Bolhuis-Versteeg, L. A. M.; Winnubst, L.; Hempenius, M. A.; Benes, N. E.; Wessling, M.; Stamatialis, D. *J. Membr. Sci.* **2011**, *372*, 182.
38. Vankelecom, I. J. F.; Moermans, B.; Verschueren, G.; Jacobs, P. A. *J. Membr. Sci.* **1999**, *158*, 289.
39. Leitner, L.; Harscoatt-Schiavo, C.; Vallières, C. *Polym. Test.* **2014**, *33*, 88.
40. Soltanieh, M.; Gill, W. *Chem. Eng. Commun.* **1981**, *12*, 279.
41. Bowen, W. R.; Mohammas, A. W.; Hilal, N.; *J. Membr. Sci.* **1997**, *126*, 91.
42. Bowen, W. R.; Welfoot, J. S. *Chem. Eng. Sci.* **2002**, *57*, 1393.
43. See-Toh, Y. H.; Silva, M.; Livingston, A. G. *J. Membr. Sci.* **2008**, *324*, 220.
44. Stawikowska, J.; Kim, J. F.; Livingston, A. G. *Chem. Eng. Sci.* **2013**, *97*, 81.
45. Bowen, W. R.; Mohammad, A. W. *A.I.Ch.E. J.* **1998**, *44*, 1799.
46. Schiller, R. *Radiat. Phys. Chem.* **1991**, *37*, 549.
47. Wilke, C. R.; Chang, P. C. *Am. Inst. Chem. Eng. J.* **1955**, *1*, 264.
48. Fedors, R. F. *Polym. Eng. Sci.* **1974**, *14*, 147.
49. Robinson, J. P.; Tarleton, E. S.; Millington, C. R.; Nijmeijer, A. *J. Membr. Sci.* **2004**, *230*, 29.
50. Seethapathy, S.; Gorecki, T. *Anal. Chim. Acta* **2012**, *750*, 48.
51. Zhang, Q.; Yuan, Q. *Sep. Sci. Technol.* **2009**, *44*, 3239.